

Selected Paper

One-Step Electrochemical Cyanation Reaction of Pyrene in Polymer Microchannel-Electrode Chips

Kosei Ueno, Fumihiko Kitagawa,† and Noboru Kitamura*

Division of Chemistry, Graduate School of Science, Hokkaido University, Sapporo 060-0810

Received October 20, 2003; E-mail: kitamura@sci.hokudai.ac.jp

Polymer microchannel chips (100 μm width × 20 μm depth) integrated with electrodes were fabricated and applied to a one-step electrochemical cyanation reaction of pyrene (PyH). An acetonitrile solution of PyH containing tetrabutylammonium perchlorate and an aqueous NaCN solution were brought into the chip by pressure-driven flow, PyH was then oxidized at the working band electrode in the channel (1.5 V vs Ag). Under the optimum conditions, 1-cyanopyrene (PyCN) was produced very efficiently in the microchannel: 61% yield. It was also confirmed that, although 1,3-dicyanopyrene ($Py(CN)_2$) was produced by bulk electrolysis (14% yield), its yield decreased to 4% in the microchip, with the $PyCN/Py(CN)_2$ yield ratio being 2.9 or 15.3 for the bulk or chip experiments, respectively. In the case of an oil/water interfacial reaction system, a propylene carbonate solution of PyH and an aqueous NaCN solution were introduced to the channel, where an electrochemical cyanation reaction of PyH analogous to that mentioned above was conducted. The interfacial reaction in the microchip was successful and the yield of PyCN as the sole product was shown to be controlled by both the flow rate and the electrode position in the chip. In-situ space-resolved absorption spectroscopy of the electrochemical intermediate in the channel chip was also conducted to allow discussion of the reaction mechanisms.

Various microfluidic devices fabricated by semiconductor micromachining technologies have been applied successfully to develop miniaturized analytical and/or chemical systems (μ-TAS).[1–3] These devices have also received broad interest as an organic synthetic microreactor integrated on a single chip.[4,5] Microreaction systems offer many advantages over traditional large-scale organic synthetic systems: efficient mass-transfer, highly effective heat management, a high specific surface (interface) area, decreases of waste and toxicity in chemical reactions, and so on.[4] Therefore, further progress in the relevant research fields is absolutely necessary. Microreactor chips so far reported have been applied mainly to biological and thermal reactions with typical examples being an enzymatic reaction,[6–8] a polymerase chain reaction,[9–11] and an organic synthetic reaction.[12–14] These studies demonstrate explicitly that microreactor chips are quite novel and, exhibit great possibilities for the chemistry of the next generation.

Among various synthetic reactions, electroorganic synthesis will be one of the most appropriate chemical reactions applied to a microsystem, since a reactant in a microchannel device integrated with an electrode(s) is electrolyzed very efficiently as compared to that in a bulk system, owing to confinement of the solute to the minute space in the vicinity of the electrode in the channel. A subsequent side reaction of an electrolyzed specimen will be reduced by one-directional solution flow in a microchannel; this has a possibility to control the product selectivity. In practice, Ehrfeld and his co-workers first proposed such a concept of an electrochemical microreactor.[15] However, the number of the fundamental studies along this line is still very few. On the basis of these characteristics, therefore, the research relevant to an electroorganic synthesis in a microchannel chip is worth exploring further and in more detail.

In the past few years, several research groups have demonstrated that microchannel chips integrated with electrodes could be applied to electrochemical detection devices for electrophoresis,[16,17] electrogenerated chemiluminescence,[18,19] and electrochemical studies in minute dimensions.[20] We also reported recently that an imprinting method first proposed by Martynova et al.[21] could be applied successfully to fabricating a polymer-based microchannel-microelectrode chip.[22,23] Fabrication of a polymer channel-electrode chip is very simple and does not need special facilities (i.e., clean room or etching apparatus). Furthermore, the chip can be duplicated very easily by a single template. Therefore, a polymer microchannel-electrode chip is expected to be applicable to an electroorganic synthetic reactor as well.

In order to demonstrate the high potentials of a polymer microchannel-electrode chip, we explored an electrochemical cyanation reaction of pyrene (PyH). The background of the present research is as follows. We reported recently an efficient interfacial one-step photocyanation reaction of PyH in microsystems: in an oil-in-water emulsion system and in a microchannel chip.[24,25] In these reports, we demonstrated that the photocyanation reaction proceeded via the pyrene cation radical produced by a photoinduced electron transfer reaction with an electron acceptor. The PyH cation radical produced is reacted with a cyanated ion present in the system, producing 1-cyanopyrene. In the case of an electrochemical cyanation reaction, if the pyrene cation radical generated at an electrode would be subjected to a nucleophilic attack by a cyanide ion, as in the case of photocyanation of pyrene mentioned above, we expect that an electrochemical cyanation reaction of PyH would pro-

† Present address: Department of Material Chemistry, Graduate School of Engineering, Kyoto University, Kyotodaigaku Katsura, Nishikyo-ku, Kyoto 615-8510

Published on the web July 9, 2004; DOI 10.1246/bcsj.77.1331

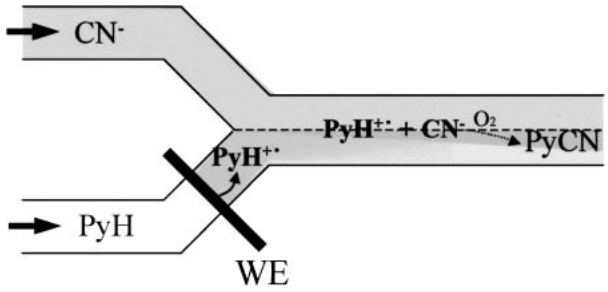

Scheme 1. Electrochemical cyanation reaction of PyH in a microchannel (Chip B).

ceed along the solution flow in a microchannel-electrode chip, as illustrated in Scheme 1.

In the present study, we fabricated polystyrene microchannel chips integrated with plural electrodes and applied the chips to electrochemical cyanation of PyH. The product yield and selectivity will be governed by various factors, so that a systematic study on the present synthetic reaction was conducted as a function of a solution-flow rate and channel-electrode geometries. In order to discuss the reaction mechanisms, the appearance of the reaction intermediate was followed simultaneously by in-situ space-resolved absorption spectroscopy.

Experimental

Chemicals. Pyrene (PyH, Wako Pure Chemical Industrial Co., Ltd.) was purified by repeated recrystallizations from ethanol. Propylene carbonate (PC, Tokyo Kasei Kogyo Co., Ltd., GR Grade) was purified by vacuum distillation in the presence of CaH_2. Acetonitrile (AN, Dojindo Laboratories, 99+%) was used without further purification. Tetrabutylammonium perchlorate (TBAP, Tokyo Kasei Kogyo Co., Ltd., GR Grade) was purified by repeated recrystallizations from acetone/diethyl ether, and was used as a supporting electrolyte throughout the study. Water was purified by distillation and deionization prior to use (GSR-200, Advantec Toyo Co., Ltd.). Sample solutions were deaerated thoroughly by purging with an Ar gas stream for 20 min prior to experiments.

Fabrication of Polymer Channel-Electrode Chip. Polymer microchannel-electrode chips were fabricated by photolithography and an imprinting method. A fabricated polymer microchip was composed of channel and electrode substrates. A commercially available polystyrene substrate (Tamiya Inc.) was used in this study as chip material. The use of a polymer substrate is very versatile, but disadvantageous because of low ability to resist organic solvents. Such characteristics were improved after an amorphous fluorocarbon resin (Cytop, Asahi Glass Co., Ltd.) was spin-coated onto the polystyrene substrate for fluorination of the surface prior to use. A silicon template for imprinting was fabricated by photolithography and dry etching techniques, as reported previously.[25] For fabrication of a channel substrate, the silicon template and the fluorinated polystyrene substrate (15 × 30 mm) were fastened tightly between two pieces of a glass plate and heated at 110 °C for 25 min to transfer the embossed structure of the template to the polymer plate. In the present study, the width, depth, and total length of the fabricated double Y-structured microchannel were set at 100 μm, 20 μm, and 60 mm, respectively.

An electrode substrate was also fabricated by an imprinting method. In the present experiments, a Pt or Ag foil with the thickness of 100 μm was used as an electrode material. A piece of foil with the width of 500 μm and the length of 10.0 mm was cut and,

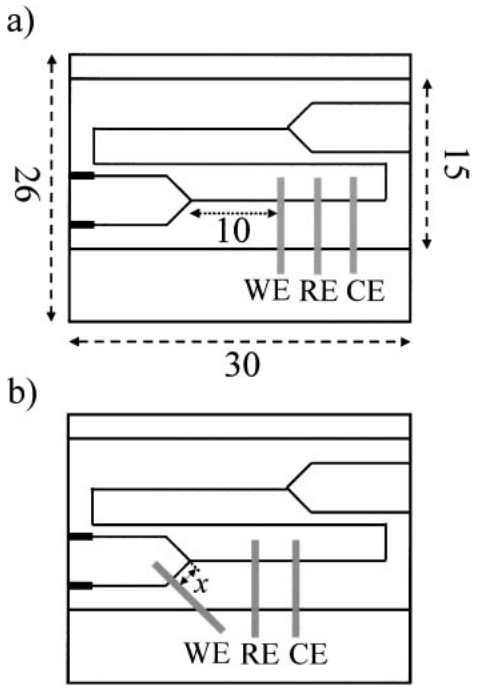

Fig. 1. Structural layouts of the microchannel chip integrated with electrodes. WE, CE, and RE represent working, counter, and reference electrodes, respectively. The sizes in the figure are shown in mm. *x* in b) represents the distance between the channel junction and the position of the WE edge. See also the main text.

the two pieces of the Pt foil (as working (WE) and counter electrodes (CE)) and one piece of the Ag foil (as a reference electrode (RE)) were put at appropriate positions on a fluorinated polystyrene substrate (26 × 30 mm). The three metal pieces and the fluorinated polystyrene substrate were then fastened tightly between two glass plates and heated at 110 °C for 25 min to bury the electrodes into the polymer substrate. Introduction of the electrodes into the polymer and their positions on the substrate were confirmed by observation under an optical microscope (Nikon Co., Optiphoto-2). Finally, the electrode substrate was covered and bonded with the channel substrate by pressing the two substrates between two glass plates at 110 °C for 18 min. The electrodes with the width of 500 μm were fabricated perpendicularly to the direction of the channel length; thus, the lengths of the electrodes were equal to the channel width: 100 μm.

In the experiments, we fabricated two types of microchannel-electrode chips: one for homogeneous electrochemical cyanation of PyH (Fig. 1a, Chip A) and the other for water/oil interfacial electrochemical cyanation of PyH (Fig. 1b, Chip B). In the case of Chip A, the WE was set at 10 mm in the downstream-side of the channel junction, while that in Chip B was integrated into the oil-phase channel in the upstream-side of the channel junction. The position of the WE in the channel (*x*) was varied as illustrated in Fig. 1b.

Electrochemical and Spectroelectrochemical Experiments. A solution flow system analogous to that reported previously was employed in the present study.[26,27] A syringe pump (Harvard Co., model 44) was used to control the flow velocity in the microchannel. The connections between the electrodes and an electrochemical analyzer (ALS, model 701A) via lead wires were made by a silver paste as an electroconductive adhesive, and connections

were fixed with an epoxy resin. For an electrochemical reaction, a potential was applied to the WE by using the electrochemical analyzer. For product analysis, the sample solutions collected from the exits of the microchannel chip were analyzed by GC–MS (Shimadzu Co., QP-5000). The absolute yields of 1-cyanopyrene (PyCN) and 1,3-dicyanopyrene ($Py(CN)_2$) as the products of the electrochemical reaction were determined on the basis of the calibration curves obtained by GC analysis of the relevant authentic sample.[24] For large-scale electrochemical experiments, a Pt electrode with the surface area of 480 cm^2 was used as WE, while Pt and Ag wires were employed as CE and RE, respectively. The sample solution in a beaker (300 mL) was stirred by using a magnetic stirrer during the reaction.

Spectroelectrochemical measurements for monitoring the PyH cation radical produced at the WE integrated in the chip were conducted by using an absorption microspectroscopy system reported previously.[28] A Xe light beam (Hamamatsu Photonics, L2274) that had been passed through a pinhole (ϕ100 μm) was introduced to an optical microscope (Nikon, Optiphoto-2) and irradiated onto a microchannel chip. In the present experiments, the paraxial ray of a microscope objective (×100, NA = 0.75) was used as a quasi-parallel probe beam, and its diameter was adjusted to ~2 μm. The beam that was passed through a sample solution in the channel chip (intensity, I) and a condenser lens was reflected by a half mirror set under the microscope stage and, then led to a multichannel photodetector (Hamamatsu Photonics, PMA-11) via an optical fiber to record an absorption spectrum. The incident light intensity of the Xe beam (I_0) was determined under analogous optical conditions for a solution without a solute.[29]

Results and Discussion

Electrochemical Cyanation Reaction of PyH. Large-Scale Experiments: An aqueous AN solution (25/25 mL) containing PyH (1.5 mM), NaCN (0.5 M), and TBAP (0.05 M) was electrolyzed at 1.5 V (vs Ag) for 1 h. Under the present experimental conditions, PyH was electrolyzed completely with a reaction time of 1 h, as confirmed by GC–MS analyses of the reaction mixture. Figure 2 shows the gas chromatograms of the reaction mixtures extracted with chloroform before (solid line) and after the electrochemical reaction (dotted line). Disappearance of the peak responsible for PyH at the retention time (t_r) of 11.8 min upon electrolysis accompanies an appearance of two new peaks at t_r = 13.0 and 14.0 min. The t_r values agreed very well with those of authentic PyCN and $Py(CN)_2$, and the mass numbers of the compounds at t_r = 13.0 and 14.0 min are 227 (PyCN) and 252 ($Py(CN)_2$), respectively. The calibration curves for PyCN and $Py(CN)_2$ made by separate experiments indicate that the absolute PyCN and $Py(CN)_2$ yields under the conditions mentioned above are 41% and 14%, respectively. On the basis of these results, we conclude that one-step electrochemical cyanation reaction of PyH proceeds in moderate yields.

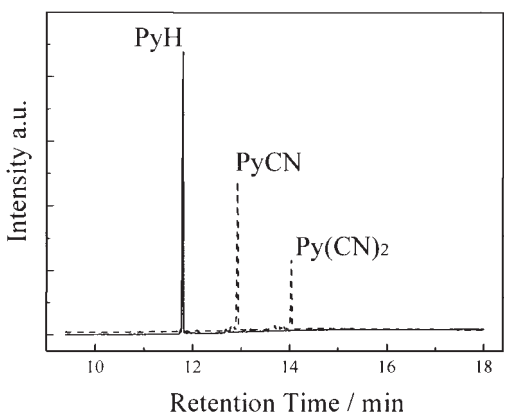

Fig. 2. Gas chromatograms of the reaction mixtures before (solid line) and after the electrochemical reaction (dotted line).

Previously, we reported that one-pot and efficient cyanation of PyH was attained by a photoinduced electron transfer (PET) mechanism, in which the PyH cation radical produced by PET between the excited singlet-state of PyH and an electron acceptor in a polar medium was subjected to a nucleophilic attack by a cyanide ion, and the subsequent oxidation of the cyanated pyrenyl radical gave PyCN.[24,25] Under the present experimental conditions, the oxidation potential of PyH in an aqueous AN solution is determined to be 1.4 V (vs Ag). At the applied voltage to the WE (V) of 1.5 V, therefore, PyH should be oxidized efficiently, producing the cation radical of PyH. Under analogous conditions, furthermore, we confirmed formation of the PyH cation radical as shown by a spectroelectrochemical study as described later. Therefore, we conclude that the PyH cation radical produced at the WE is subjected to a nucleophilic attack by a cyanide ion and subsequent oxidation of the radical gives PyCN, similar to the photocyanation reaction of PyH mentioned above.

On the other hand, $Py(CN)_2$ is produced by the electrochemical reaction, while production by the photoreaction has not been confirmed. One possible reason for formation of $Py(CN)_2$ in the present experiments might be participation of a CN radical and/or dicyan (cyanogen, $(CN)_2$) produced by direct oxidation of a cyanide ion at the WE. When the CN radical and/or $(CN)_2$ are produced, these species would attack PyH via a radical mechanism, producing $Py(CN)_2$. Under the present conditions, however, a cyanide ion is not electrolyzed, since no current has been observed at the WE during electrolysis (V = 1.5 V) of an aqueous NaCN solution. Therefore, the contribution of the CN radical and/or dicyan to $Py(CN)_2$ formation is denied.

Another possible origin of formation of $Py(CN)_2$ will be two-electron oxidation of PyH and/or one-electron oxidation of PyCN, giving the dication of PyH (PyH^{2+}) and/or the radical cation of PyCN ($PyCN^{+\bullet}$), respectively. In practice, the electrode potentials of $E(PyH/PyH^{2+})$ and $E(PyCN/PyCN^{+\bullet})$ were 1.55 and 1.51 V (vs Ag), respectively, as estimated by cyclic voltammetry. At V = 1.5 V, therefore, both PyH^{2+} and $PyCN^{+\bullet}$ are likely to produce simultaneously during the electrolysis, and subsequent nucleophilic attack by a cyanide ion(s) will afford $Py(CN)_2$.

In the present experiments, the absolute PyCN and $Py(CN)_2$ yields depended slightly on the applied potential to the WE, since the electrode potentials of $E(PyH/PyH^{+\bullet})$, $E(PyH/PyH^{2+})$, and $E(PyCN/PyCN^{+\bullet})$ were very close with one another. At V = 1.4 V (vs Ag), in practice, the absolute PyCN and $Py(CN)_2$ yields were 39% and 9%, respectively, while those at V = 1.6 V (vs Ag) were 37% and 12%, respectively. The cyanation yields were the highest at V = 1.5 V (vs Ag) in the V range studied. Therefore, we set V at 1.5 V (vs Ag) throughout the present studies.

Electrochemical Cyanation Reaction of PyH in the Microchannel-Electrode Chip. Since we had succeeded in one-step electrochemical cyanation of PyH by bulk experiments, the reaction system was applied to the microchannel-electrode chip. An aqueous NaCN solution (1 M) and an AN solution containing PyH (3 mM) and TBAP (0.1 M) were introduced separately to a double Y-type microchannel-electrode chip (Chip A, see also Fig. 1a) with the same flow velocity ($u = 0.05$ μL min^{-1}), and the potential ($V = 1.5$ V) was applied to the WE. It is worth pointing out that, in a microchannel, two miscible solutions are not mixed simultaneously at the channel junction owing to the solution-flow characteristics in a microchannel: laminar flow.[30,31] In order to allow mixing two solutions and subsequent electrochemical oxidation of PyH, therefore, we set the WE at 10 mm in the downstream-side of the channel junction.

Figure 3 shows the gas chromatograms of the reaction mixtures before (solid line) and after the reaction (dotted line), where the latter solution was collected from the exit of the microchannel. As in the case for the large-scale experiments, it was confirmed that the decrease in the PyH peak intensity resulted in an appearance of the PyCN and $Py(CN)_2$ peaks. The absolute PyCN and $Py(CN)_2$ yields were 61% and 4%, respectively. For the chip experiments, the reaction time (t) is determined by the electrolysis time of the reactant solution in the microchannel; electrolysis time = electrode width (0.5 mm)/average linear flow velocity (mm s^{-1}). At $u = 0.05$ μL min^{-1}, as an example, t is calculated to be 1.2 s. It is worth emphasizing that, although the PyCN yield is 41% for the large-scale experiments with the reaction time of 1 h (Fig. 2), a yield of 61% has been attained by the microchannel chip with the reaction time as short as 1.2 s. Although the data are not shown here, the PyCN yield increased from 17% to 61% with decreasing the solution-flow rate from 0.15 to 0.05 μL min^{-1}. The slower the flow rate is the more the number of PyH oxidized at the WE. Therefore, the yield increases with decreasing the flow rate. Futhermore, electrolysis of PyH at the WE in the microchannel proceeds more efficiently than that in a bulk system. In a microchip, namely, the diffusion length of a solute is limited by the presence of the channel wall above the WE, leading to very efficient mass feed to the electrode. On the other hand, mass feed to the WE in a bulk system is governed essentially by the mass transport rate of PyH and diffusion length around the WE is much longer than that in a microchip. Therefore, the superior PyCN yield observed by the chip over that observed by the bulk experiments is a reasonable consequence; this is one of the important aspects in the electrochemical reaction in a microchip.

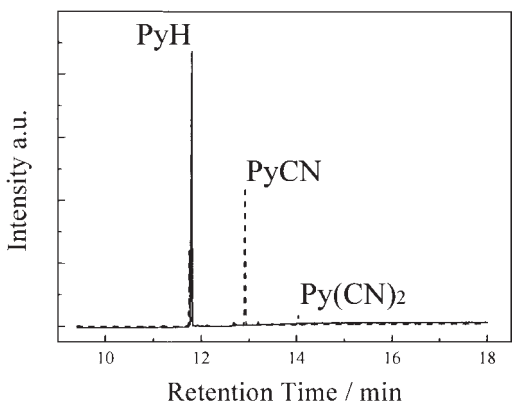

Fig. 3. Gas chromatograms of the reaction mixtures before (solid line) and after the reaction (dotted line). The reaction mixture was collected from the exit of the microchannel-electrode chip (Chip A).

Another important result found in the chip experiments is the lower $Py(CN)_2$ yield (4% at 0.05 μL min^{-1}) as compared to that in the bulk system: 14%. This is among the very important characteristics of the present reaction in the microchannel, and the product selectivity has been shown to be much improved by the use of the microchannel: the ratio of the PyCN yield to the $Py(CN)_2$ yield in the chip or bulk experiments is 15.3 or 2.9, respectively. Also, the results provide information about the reaction mechanisms. In bulk electrolysis, namely, PyCN once produced has many chances to be oxidized again producing $PyCN^{+\bullet}$. Therefore, $Py(CN)_2$ is likely to be produced by the reaction between $PyCN^{+\bullet}$ and a cyanide ion. However, the probability of reoxidation of PyCN is very low in the microchip, since the electrolyzed solution is driven away to the downstream-side of the WE. The lower $Py(CN)_2$ yield found by the chip experiments compared to that found by the bulk electrolysis thus suggests that the mechanistic origin of formation of $Py(CN)_2$ is cyanation of the PyCN radical cation, though the conclusive evidence has not been obtained yet. These results and discussions demonstrate that both the reaction yield and the product selectivity can be controlled by the solution-flow velocity in the microchannel-electrode chip; such control cannot be realized by bulk electrolysis.

Electrochemical Cyanation Reaction of PyH at the Oil/Water Interface in the Microchannel-Electrode Chip. For further demonstration of the characteristics of the microchip chemistry, we conducted an oil/water interfacial electrochemical cyanation reaction of PyH in a microchip. In the oil/water reaction system, we anticipated that the following processes would proceed in a microchannel (see Scheme 1). Under laminar flow of an aqueous NaCN solution and an immisible oil containing PyH and TBAP in a microchannel, electrolysis of PyH is conducted in the oil phase. In order to achieve this, we used Chip B (Fig. 1b), in which the WE was set in the upstream-side of the channel junction. The cation radical of PyH generated at the WE is driven to the water/oil interface at the junction by pressure-driven flow and would be subjected to a nucleophilic attack by a cyanide ion at the interface, producing PyCN. Since the solubility of PyCN in water is very poor, PyCN will be distributed to the oil phase along solution flow in the microchannel (i.e., extraction).[25]

Experimentally, an aqueous NaCN solution (1 M) and a propylene carbonate (PC) solution of PyH (3 mM)/TBAP (0.1 M) were introduced separately into the Y-structured microchannel-electrode chip with the same flow velocity ($u = 0.2$ μL min^{-1}). After confirmation of the formation of a stable oil/water interface in the channel, a potential ($V = 1.5$ V (vs Ag)) was applied to the WE set at the channel junction ($x = 0$ mm) as shown in Fig. 4; x is defined as the distance from the junction to an arbitrary position in the oil phase channel in the upstream-side (see also, Fig. 1b). In the experiments, the solution-flow rate (u) was set faster than 0.2 μL min^{-1} to construct stable and parallel oil/water streams in the microchannel (i.e, in the microchannel be-

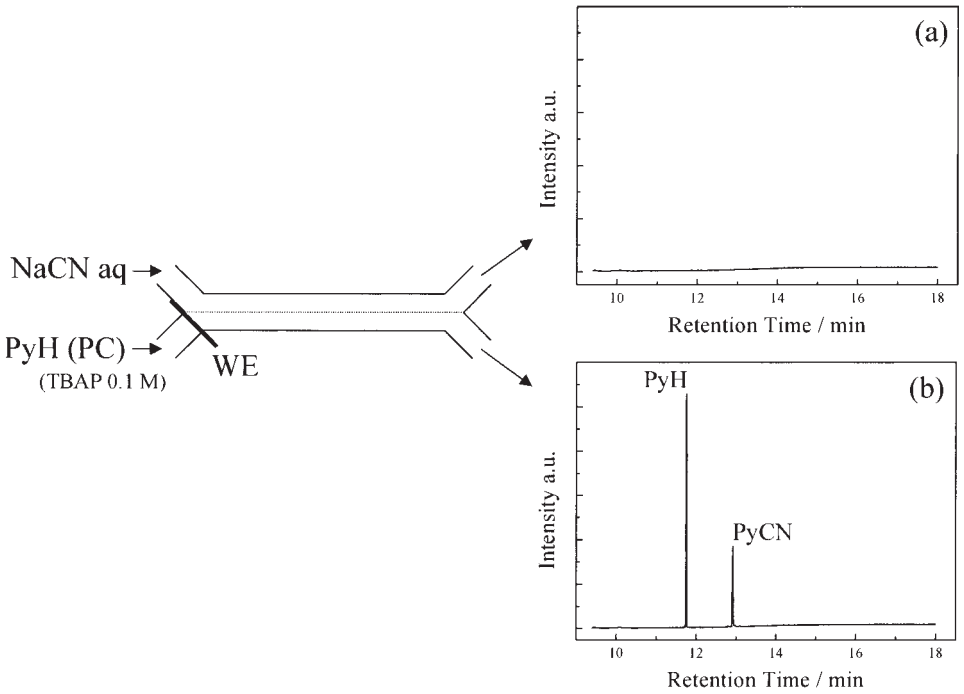

Fig. 4. Gas chromatograms of the water (a) and oil phases (b) after the electrochemical reaction in the microchannel-electrode chip (Chip B).

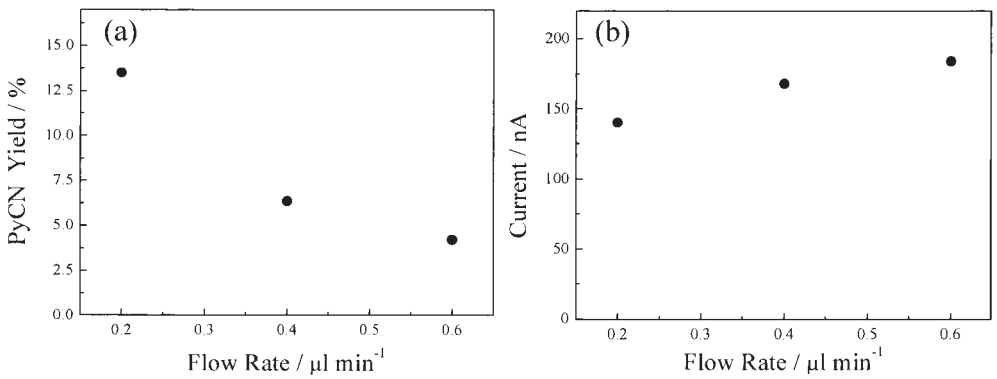

Fig. 5. Solution-flow velocity dependences of the absolute PyCN yield (a) and the steady-state current observed at WE (b) in the microchannel-electrode chip (Chip B).

tween the entrance and exit junctions).

Figure 4 shows the gas chromatograms of the water (a) and oil phases (b), which were collected from the exits of the microchip. It is seen clearly that PyCN is obtained exclusively from the oil phase, demonstrating that PyCN produced electrochemically is extracted to the PC phase during two-phase laminar flow in the microchannel. In practice, the two phases were separated completely even at the exit of the microchannel, as confirmed by observation under a microscope.[25,32] The chromatogram in Fig. 4b also demonstrates that PyCN is produced selectively without formation of $Py(CN)_2$, though the PyCN yield of 13.5% is lower than that obtained by Chip A: Fig. 2. Since the electrode is set at $x = 0$ before the confluence of the two solutions, a PyH cation radical alone is generated at the electrode; this is subjected to a cyanation reaction at the interface. In the case of the homogeneous electrochemical cyanation by using Chip A (Figs. 2 and 3), the cation radical of PyCN would be more or less oxidized again producing $Py(CN)_2$ (4%), as discussed before. However, such a possibility is absent in the case of Chip B. Therefore, PyCN is produced exclusively by using Chip B. In addition, it was confirmed that PyCN was the sole product irrespective of the applied potential (1.3–1.7 V (vs Ag)), while the PyCN yield depended on V. It is worth noting, furthermore, that u is set at 0.2 μL min^{-1} for the experiments in Fig. 4; this value is faster than those in Figs. 2 and 3. One of the primary reasons for the lower PyCN yield as compared to that by Chip A is a faster solution-flow velocity and, this can be improved by the dimensions of the channel structures. On the basis of these discussions, we conclude that the electrochemical cyanation reaction of PyH proceeds successfully at the PC/water interface in the microchannel as illustrated in Scheme 1.

Analogous experiments to those in Fig. 4 were also performed at different u values to elucidate the relationship between u and the PyCN yield. The u dependence of the absolute PyCN yield is summarized in Fig. 5(a). The results demonstrate clearly that the reaction yield increases from 4.2% to 13.5% on

decreasing u from 0.6 to 0.2 μL min^{-1}. This indicates that the electrochemical cyanation reaction of PyH can be controlled by the solution-flow rate in the microchannel. Furthermore, it is supposed that the relationship between u and the PyCN yield should be related closely to the electric charge flowing at the electrode. The u dependence of the steady-state current at the WE was then studied by chronoamperometry. As shown in Fig. 5(b), the steady-state current observed at the WE exhibited very small u dependence. The results indicate that the u values studied are too fast; this results in over-feed of PyH to the WE. Therefore, the current is limited by the charge transfer rate of PyH at the WE, demonstrating that the efficiency of the PyH electrolysis at each u is almost constant in a unit time. The amount of the PyH cation radical generated at the WE per unit volume thus decreases in proportion to the inverse of u, leading to the u dependence of the PyCN yield in Fig. 5(a). It is concluded that the u dependence of the PyCN yield is explained very well by the amount of PyH oxidized at the WE.

Spatial Modulation of the PyCN Yield. One of the important aspects in the present polymer microchannel-electrode chip is the fact that arbitrary-designed polymer channel-electrode chips can be fabricated very easily. As an example, when the spatial position of the WE in the microchannel is modulated arbitrary, this might influence the PyCN yield. If this is the case, one can control the reaction yield by spatial arrangements of both WE and the microchannel. In order to test such an idea, we fabricated several channel-electrode chips with the position of the WE in the oil phase being varied by x: $x = 0.0$ to -2.0 in Fig. 1b. Then, we studied a WE position dependence of the PyCN yield; the results are shown in Fig. 6. It is seen clearly from the Fig. 6 that the PyCN yield decreases with shifting the WE position toward the upstream-side (i.e, x from 0 to -2 mm), and the electrochemical cyanation reaction does not proceed at $x = -2.0$ mm. This is readily understood by the fact that the PyH cation radical generated at the WE is deactivated more or less before it reacts with a cyanide ion at the oil/water interface in the microchannel. Clearly, the efficiency of the cation radical reaching the interface becomes lower with shifting the WE to more negative direction in x: toward the upstream-side of the junction.

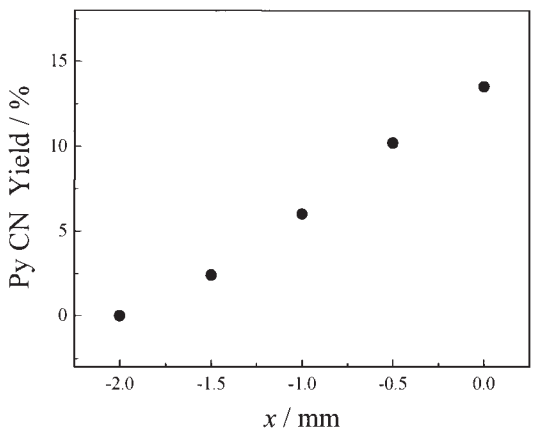

Fig. 6. WE position (x) dependence of the absolute PyCN yield.

The above discussions indicate that the lifetime of the PyH radical cation generated at the WE is short and that the radical cation should deactivate along with solution-flow. In order to confirm this directly, we explored a spectroelectrochemical study by using the microchannel-electrode chip. Experimentally, the absorption spectra of the oil phase at several positions in the vicinity of the WE ($x = -2.5$ to 0.0 mm) were measured upon electrolysis of the solution at $V = 1.5$ V (vs Ag). In the experiments, we set the flow velocity at $u = 0.1$ μL min^{-1} to obtain the absorption spectrum with high signal-to-noise ratios. Figure 7(a) shows the absorption spectra of the oil phase observed at $x = -1.9$, -1.3, and -0.7 mm. The absorption spectrum showing the maximum wavelength (λ_{max}) at 450 nm was in good accordance with that of the PyH cation radical, observed by laser photolysis or pulse radiolysis of PyH.[33–35] This demonstrates that the PyH radical cation is produced certainly as the intermediate for the cyanation reaction of PyH.

In the present experiments, the amount of the PyH cation radical can be estimated by the total electric charge flowing at the WE. At $u = 0.1$ μL min^{-1}, chronoamperometry indicates that one-third of the PyH molecules in the solution is oxidized to the cation radical at the electrode. Knowing the molar absorption coefficient of the PyH radical cation at 450 nm to be 45000 M^{-1} cm^{-1},[36] we calculated the absorbance of the radical cation at 450 nm and $x = -2.5$, under the assumptions that the optical pathlength for absorption measurements is equal to the

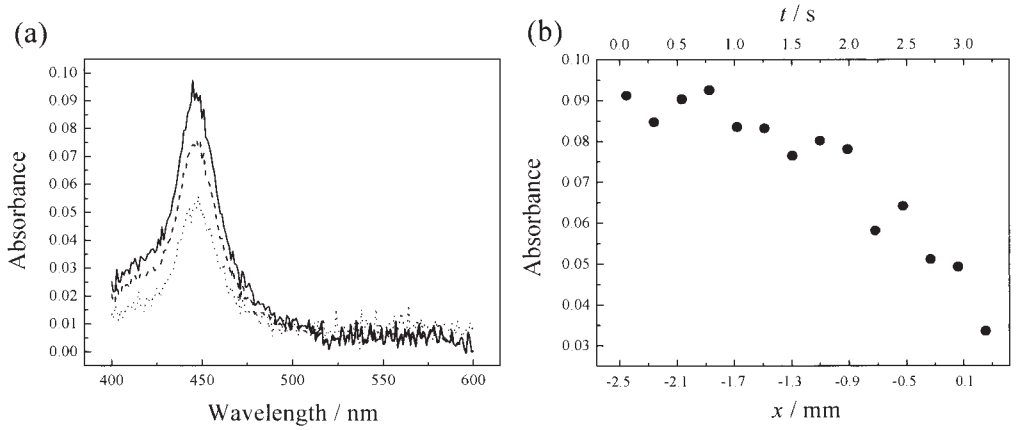

Fig. 7. (a) The absorption spectra of the oil phase observed at $x = -1.9$ (the solid line), -1.3 (the broken line), and -0.7 mm (the dashed line). (b) The x dependence of the absorbance at 450 nm.

channel depth (20 μm) and the one-third of PyH in the sample solution (3 mM) is oxidized at the WE. The calculated value of 0.09 was in good agreement with the observed absorbance in Fig. 7(a): 0.09. Correct and precise absorption measurements have been shown to be conducted by the present spectroelectrochemical system and we conclude that quantitative discussions on the cyanation reaction can be done on the basis of the spectroelectrochemical data.

Analogous experiments to those in Fig. 7(a) were then conducted at various x and, the x dependence of the absorbance at 450 nm is summarized in Fig. 7(b). Although the data were somewhat scattered, the absorbance at 450 nm was almost constant at around 0.09 in the x range of -2.5 to -1.9 mm. In this x range, therefore, the concentration of the cation radical is in the steady-state, in which mass (i.e., cation radical) feed to each position is balanced with deactivation of the cation radical, since the electrolyzed solution is provided continuously to each x position from the upstream side of the channel. At $x > -1.7$ mm, however, the absorbance of the cation radical decreased gradually with x. Since the flow velocity (u) is fixed at a constant value, the positional (x) data in Fig. 7(b) are converted very easily to the temporal data ($t = x/u$), as the temporal scale is included in Fig. 7(b). The data demonstrate that the absorbance of the cation radical decreased gradually in the t range of 1–3 s; therefore, the lifetime of the PyH cation radical is evaluated to be in the order of several seconds. It is confirmed, therefore, that the decrease in the PyCN yield with shifting the WE position toward the upstream-side is due to deactivation of the PyH cation radical generated at the WE before it reacts with a cyanide ion at the oil/water interface in the microchannel. The PyCN yield is thus controllable by the use of a microchannel-electrode chip.

Conclusion

In this work, we fabricated two types of a microchannel-electrode chip: one for electrochemical cyanation of PyH in a homogeneous aqueous AN solution (Chip A) and the other for that at a water/propylene carbonate interface (Chip B). In both cases, PyCN was confirmed to be produced in a moderate yield even by the reaction in the microchannel. Furthermore, 1,3-dicyanopyrene is also produced under certain conditions. As one of the important results, however, the product selectivity (PyCN:Py$(CN)_2$) was shown to be controlled by both the experimental mode (Chip A or B) and the solution-flow velocity. In the case of the experiments with Chip B (interfacial system), PyCN as the sole product was obtained exclusively from the oil phase, demonstrating that the chip can be utilized as an automated electrochemical reactor. Furthermore, the PyCN yield was modulated by both the position of the WE in the microchannel and the solution-flow velocity. These cannot be done by a conventional bulk experiment. The present results thus demonstrate the high potentials of a microchannel-electrode chip. We are sure that various new research fields could be developed by the use of microchannel chips.

N.K. is grateful for Grant-in-Aids from the Ministry of Education, Culture, Sports, Science and Technology (nos. 13853004 and 14050001) for financial support of the research. K.U. also acknowledges JSPS for a fellowship.

References

1 "Microsystem Technology in Chemistry and Life Science," ed by A. Manz and H. Becker, Springer-Verlag, Berlin (1999).

2 "Micro Total Analysis Systems '98," ed by D. J. Harrison and A. Van Den Berg, Kluwer Academic Publishers, Dordrecht (1998).

3 "Micro Total Analysis Systems 2002," ed by Y. Baba, S. Shoji, and A. Van Den Berg, Kluwer Academic Publishers, Dordrecht (2002).

4 "Microreaction Technology: Industrial Prospects," ed by W. Ehrfeld, Springer Verlag, Berlin (1999).

5 "Microreactors: New Technology for Modern Chemistry," ed by W. Ehrfeld, V. Hessel, and H. Löwe, WILEY-VCH Verlag, Weinheim (2000).

6 Y. Lv, Z. Zhang, and F. Chen, *Analyst*, **127**, 1176 (2002).

7 D. S. Peterson, T. Rohr, F. Svec, and J. M. J. Fréchet, *Anal. Chem.*, **74**, 4081 (2002).

8 J. Heo, K. J. Thomas, G. H. Seong, and R. M. Crooks, *Anal. Chem.*, **75**, 22 (2003).

9 E. T. Lagally, P. C. Simpson, and R. A. Mathies, *Sens. Actuators, B*, **63**, 138 (2000).

10 J. Khandurina, T. E. McKnight, S. C. Jacobson, L. C. Waters, R. S. Foote, and J. M. Ramsey, *Anal. Chem.*, **72**, 2995 (2000).

11 K. Sun, A. Yamaguchi, Y. Ishida, S. Matsuo, and H. Misawa, *Sens. Actuators, B*, **84**, 283 (2002).

12 H. Hisamoto, T. Saito, M. Tokeshi, A. Hibara, and T. Kitamori, *Chem. Commun.*, **2001**, 2662.

13 H. Surangalikar, X. Ouyang, and R. S. Besser, *Chem. Eng. J.*, **93**, 217 (2003).

14 A. Daridon, V. Fascio, J. Lichtenberg, R. Wütrich, H. Langen, E. Verpoorte, and N. F. de Rooij, *Fresenius' J. Anal. Chem.*, **371**, 261 (2001).

15 H. Löwe and W. Ehrfeld, *Electrochim. Acta*, **44**, 3679 (1999).

16 R. S. Martin, K. L. Ratzlaff, B. H. Huynh, and S. M. Lunte, *Anal. Chem.*, **74**, 1136 (2002).

17 D. R. Manica and A. G. Ewing, *Electrophoresis*, **23**, 3735 (2002).

18 T. Horiuchi, O. Niwa, and N. Hatakenaka, *Nature*, **394**, 659 (1998).

19 W. Zhan, J. Alvarez, and R. M. Crooks, *J. Am. Chem. Soc.*, **124**, 13265 (2002).

20 J. S. Rossier, M. A. Roberts, R. Ferrigno, and H. H. Girault, *Anal. Chem.*, **71**, 4294 (1999).

21 L. Martynova, L. E. Locascio, M. Gaitan, G. W. Kramer, R. G. Christensen, and W. A. Maccrehan, *Anal. Chem.*, **69**, 4783 (1997).

22 K. Ueno, F. Kitagawa, H.-B. Kim, T. Tokunaga, S. Matsuo, H. Misawa, and N. Kitamura, *Chem. Lett.*, **2000**, 858.

23 K. Ueno, H.-B. Kim, and N. Kitamura, *Anal. Chem.*, **75**, 2086 (2003).

24 F. Kitagawa and N. Kitamura, *J. Org. Chem.*, **67**, 2524 (2002).

25 K. Ueno, F. Kitagawa, and N. Kitamura, *Lab. Chip*, **2**, 231 (2002).

26 H.-B. Kim, K. Ueno, M. Chiba, O. Kogi, and N. Kitamura, *Anal. Sci.*, **16**, 871 (2000).

27 N. Kitamura, Y. Hosoda, C. Iwasaki, K. Ueno, and H.-B. Kim, *Langmuir*, **19**, 8484 (2003).

28 K. Ueno and N. Kitamura, *Analyst*, **128**, 1401 (2003).
29 N. Kitamura, M. Hayashi, H.-B. Kim, and K. Nakatani, *Anal. Sci.*, **12**, 49 (1996).
30 J. P. Brody, P. Yager, R. E. Goldstein, and R. H. Austin, *Biophys. J.*, **71**, 3430 (1996).
31 J. P. Brody and P. Yager, *Sens. Actuators, A*, **58**, 13 (1997).
32 K. Ueno, H.-B. Kim, and N. Kitamura, *Anal. Sci.*, **19**, 391 (2003).
33 K. H. Grellmann and A. R. Watkins, *J. Am. Chem. Soc.*, **95**, 983 (1973).
34 T. Shida and W. H. Hamill, *J. Chem. Phys.*, **44**, 4372 (1966).
35 A. Kira, S. Arai, and M. Imamura, *J. Chem. Phys.*, **54**, 4890 (1971).
36 T. Hino, H. Akazawa, H. Masuhara, and N. Mataga, *J. Phys. Chem.*, **80**, 33 (1976).